

## Strengthening Potentials of Aluminium (2.3-3.3) % and Molybdenum (0.44-1.44) % Additives on the Compressive and Tensile Strengths of Monel 400

Augustine Anyiam Oputa \*, Kennedy Chinedu Owuama, Elvis Emifoniye, Vincent Chukwuemeka Ezechukwu and P. N. Atanmo

*Department of Mechanical Engineering, Chukwuemeka Odumegwu Ojukwu University Uli Campus, Anambra State, Nigeria.*

World Journal of Advanced Research and Reviews, 2025, 27(02), 561-571

Publication history: Received on 21 June 2025; revised on 01 August; accepted on 04 August 2025

Article DOI: <https://doi.org/10.30574/wjarr.2025.27.2.2806>

### Abstract

This paper examines aluminum and molybdenum strengthening potentials on the compression and tensile strengths of Monel 400. Solute mix (Al and Mo) and optimization was determined using a design computer software. Production of research test samples was accomplishable with sand casting technique. Cast specimens were machined to ASTM and ISO standards. Machined specimens were heat to 950 °C, soaked for one hour and allowed to cool in the furnace. Test samples were loaded into the UTM, and strained to failure. Specimens test analysis indicate [(937-967), (764-787.4)] MPa, (179-183) GPa and (0.32-0.324) for compression and tensile strengths, elastic modulus and Poisson ratio. Test results apply to plot the compressive and tensile strengths graphs. Optimal compression and tensile strengths, elastic modulus and Poisson ratio of test specimens is (967, 787.4) MPa, 183.3 GPa and 0.324. Comparison of these properties results with that of Monel 400 and k500 showed a percentage increase of (27.4, 4.2) % and (27, 4) % for compressive and tensile strengths, 2.4 % for elastic modulus and 0 % for Poisson ratio. Solute (Al and Mo) adequate dissolution and occupation of the solvent interstitial sites refined grain sizes, increased grain boundaries and further restricted dislocation motion. These microstructural changes increased the research alloy internal stress and subsequent improvement in deformation requirements. Where strengths is a preference over weight to strength ratio, Monel 400 strengthened with Al and Mo is a preference over Monel 400 and or k500.

**Keywords:** Monel 400; k500; Material selection; Aluminium; Molybdenum; Compressive; Tensile strengths

### 1. Introduction

No doubt, some of the metals and alloys that have continued to remain important in technology development are molybdenum, nickel, cobalt, titanium, copper, Monel metal, etc. Monel metal has outstanding resistance to corrosion. It comes in a variant of different grades; Monel 400, 401, 403, and K500. For increased performance, k500 was created through alloying, K-500 formation result from the addition of aluminium and titanium to Monel 400. K-500 has greater strength and hardness in addition; it retains outstanding resistance to corrosion, which is typical of Monel 400. K500 tensile and yield strength is twice, and thrice higher compared to that for Monel 400. Notably the tensile strength of Monel 400 ranges between (512-620) MPa, yield strength is (172-345) MPa, and maintain an elongation of (60-35) %. K 500 tensile strength ranges between (621-758) MPa, a yield strength of (276-414) MPa, and maintain an elongation of (45-25) %. The development of K500 retained the outstanding corrosion resistance of Monel 400 with improvements in the compressive and tensile strengths from (759 and 620) MPa to (928 and 758) MPa. However, the mechanical properties of Monel 400 and k-500 do not make both choice materials in environments where strengths and elastic modulus exceed (928,759) MPa and 179 GPa especially in temperature environment above 400 °C–600°C. This is because tensile and yield strengths increase with a decrease in temperature but ductility and toughness are virtually unimpaired. There is absence of ductile-to-brittle transformation, which can take place at low temperatures such as that

\* Corresponding author: Augustine Anyiam Oputa

of liquid hydrogen. Thus, the solvent and k-500 are most suitable for many cryogenic applications and are not materials of choice for high strengths purposes typically in elevated temperature applications.

Compressive and tensile tests are the most common type of tests used to measure the mechanical properties of materials. They are widely used to provide basic design information on strength of materials and are acceptable test used to specify characteristic properties of materials. The major parameters that describe the stress-strain curve obtained during the compressive and tensile tests are the ultimate tensile strength (UTS), yield strength or yield point ( $\sigma_y$ ), elastic modulus (E), percent elongation ( $\Delta L\%$ ) and the reduction in area (RA%). Toughness, Resilience, Poisson's ratio ( $\nu$ ) can also be found by the use of this testing technique. Compressive and tensile tests measure the resistance of a material to a static or slowly applied force (GÜRBÜZ, 2005; Rajput, 2008; & Khlystov, 2013; & ASTM International, 2004; David, 2008). Compressive and tensile strength of materials is a fundamental concern measured in terms of either the stress necessary to cause appreciable plastic deformation or the maximum stress that materials can withstand. These measures of strength are used, with appropriate caution (in the form of safety factors), in engineering design. More so, a material's ductility, and elasticity, which is a measure of how much it can be deformed before it fractures is of interest (Rajput, 2010).

(Ashby 1999 & 2003; Ashby & Cebon 1993; Pradeep et al; Aldrich, 2007) observed that today we live in material world, where metals and alloys satisfy engineering services more than any or all other materials combined in mankind development for over hundreds of decades. This obviously align with the opinion of Kurzydłowski (1999) that amongst types of engineering materials, metals are the most widely used. (Kailas et al, 2007), in the materials world man lives, when making a new device/component, most often we come across a very familiar problem; the ability to select most appropriate material(s). Contemporary successes (especially in technology), lifestyle, comfort, and developments would be impossible without metals, and alloys. This is because some of the properties of metals and alloys (elastic constants, microstructures) can be directly linked to the type, and nature of metallic bonds between the atoms. More so, metals have relatively high values of elastic constants, and alloying, and proper heat treatment is useable to make them stronger. (Shields, 2013) molybdenum metal and its alloys find more and more applications, always because of its special properties, which no other material possesses or guarantee. (Tomohiro; et al, 2004), molybdenum (Mo) has many favourable properties for high-temperature structural applications because of its high point of melt (2890 K), low coefficient of thermal expansion, high thermal conductivity and excellent compatibility with liquid metals as well as high degree of fabricability by metal processing techniques. Molybdenum's strength and stability at elevated temperatures forms the pivot of most of its application. This work investigates the strengthening potentials of aluminium and molybdenum additives on the compressive and tensile strengths attribute Monel 400 by sand casting technique. Test samples are machined, heat up to 950 °C, soaked for one hour and cooled in the furnace.

## 2. Materials and Method

The materials used for this research include wood patterns, saw, bail out furnace, moulding box, synthetic moulding sand, wood turning lathe, emery paper, sand milling machine, scooper, shank, blower, books, design expert software, amongst others. Castings production is by sand casting technique. Test samples machining and annealing is with reference to ASTM and ISO standards. Annealing temperature is 950 °C; soaked for one hour, and cooled in the furnace. Specimens for tensile test incorporate a transition curve between the gripped ends and the parallel length, fig. 1a and fig. 2a. The gripped ends are circular in shape, threaded to M 10 and suits the grips of the testing machine. The axis of the test piece is parallel to the axis of application of the force. Compression test samples diameter is  $(13 \pm 0.2)$  mm, length is  $(39 \pm 1)$  mm, fig. 2b.

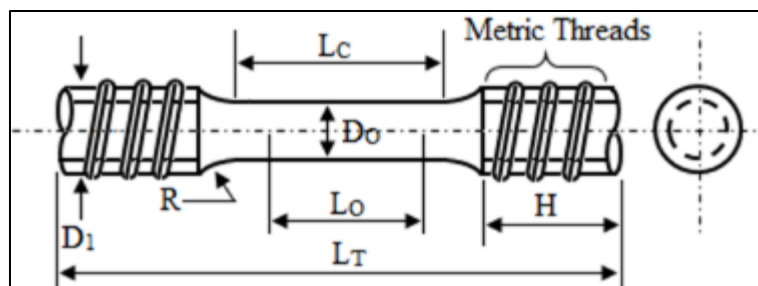


**Figure 1** (a) Tensile test sample dimension (ASTM E21, ISO 6892–part 1 to 3).  $D_0$  is the original diameter of the parallel length = 6 mm. Source: (ASTM, 2013: 20018)

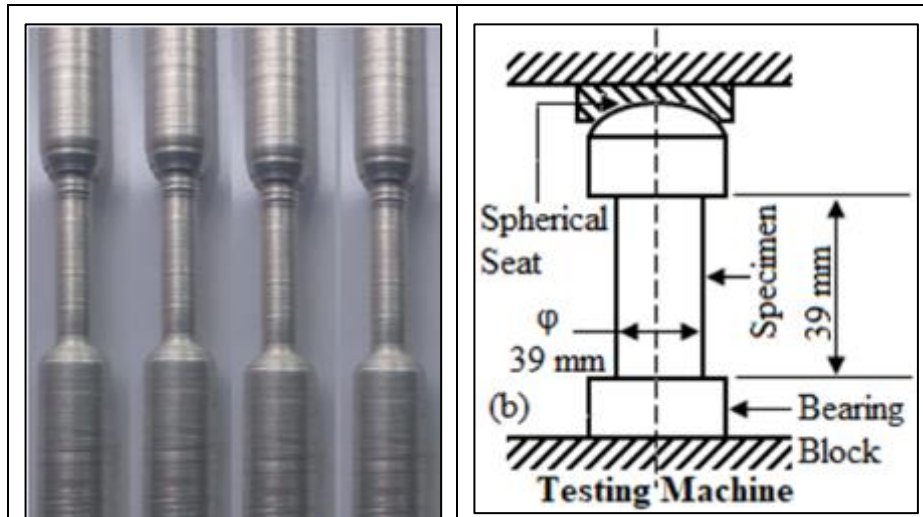


**Figure 2 (a)** Tensile test specimens. **(b)** Compressive test sample dimension (ASTM E9- E19 and E209)

Machined samples are placed into the jaws of the universal testing machine (UTM), and loads are applied appropriately. Observation of load deformations for respective specimen as displayed on a computer screen were recorded. The values and universal strength equations (3.1–3.3) was used to evaluate test samples compressive and tensile strengths, elastic modulus and Poisson ratio. Stress-strain graphs for compression and tensile strengths were plotted.

Relationships used for calculations

$$\text{Tensile stress} = \frac{\text{Max. Load (P)}}{\text{Original area (A}_0\text{)}} = \text{MPa} \quad \text{eqn. 3.1}$$

$$\text{Elastic modulus, E} = \left( \frac{\text{Stress below proportional limit}}{\text{Corresponding strain}} \right) = \text{MPa} \quad \text{eqn. 3.2}$$

$$\mu = \left( \frac{\text{Lateral(transverse)strain}}{\text{Linear (primary)strain}} \right) = \left( \frac{1}{m} \right) \quad \text{eqn. 3.3}$$

Where  $\mu$  is the Poisson's ratio,  $m$  is a constant. (Rajput, 2008 & 2010).

**Table 1** Percentage composition of the research alloy

| S/N | Element    | % Composition by weight | Remark   |
|-----|------------|-------------------------|----------|
| 1   | Nickel     | 63                      | Constant |
| 2   | Cobalt     | 5                       | Constant |
| 3   | Carbon     | 0.25                    | Constant |
| 4   | Manganese  | 1.5                     | Constant |
| 5   | Iron       | 2.0                     | Constant |
| 6   | Sulphur    | 0.01                    | Constant |
| 7   | Silicon    | 0.5                     | Constant |
| 8   | Copper     | 29                      | Constant |
| 9   | Aluminium  | 2.30 – 3.30             | Variable |
| 10  | Molybdenum | 0.44 – 1.44             | Variable |

**3. Design (Actual)**

**Table 2** Actual Design

| Run | Al  | Mo   | Compressive Strength | Tensile Strength | Elastic Modulus | Poisson Ratio |
|-----|-----|------|----------------------|------------------|-----------------|---------------|
| 1   | 2.5 | 1.44 |                      |                  |                 |               |
| 2   | 2.3 | 1.24 |                      |                  |                 |               |
| 3   | 2.7 | 0.44 |                      |                  |                 |               |
| 4   | 3.3 | 1.04 |                      |                  |                 |               |
| 5   | 2.9 | 1.44 |                      |                  |                 |               |
| 6   | 2.7 | 0.84 |                      |                  |                 |               |
| 7   | 3.3 | 1.44 |                      |                  |                 |               |
| 8   | 2.3 | 0.84 |                      |                  |                 |               |
| 9   | 2.3 | 0.44 |                      |                  |                 |               |
| 10  | 2.7 | 0.84 |                      |                  |                 |               |
| 11  | 2.7 | 0.84 |                      |                  |                 |               |
| 12  | 3.3 | 1.04 |                      |                  |                 |               |
| 13  | 2.5 | 0.64 |                      |                  |                 |               |
| 14  | 3.1 | 0.44 |                      |                  |                 |               |
| 15  | 3.1 | 0.44 |                      |                  |                 |               |
| 16  | 2.7 | 0.84 |                      |                  |                 |               |

**4. Result**

This result of the research is as shown in table 3.1 to below

**Table 3** Compressive strength and elastic moduli

| Run | Limit of Prop. (MPa) | Elastic Limit (MPa) | Comp. Strength (MPa) | Fracture Strength | Strength Below Prop. Limit (MPa) | Poisson Ratio | Young Modulus; E (GPa) |
|-----|----------------------|---------------------|----------------------|-------------------|----------------------------------|---------------|------------------------|
| 1   | 470                  | 650                 | 964                  | 700               | 337.7192982                      | 0.3212        | 183                    |
| 2   | 464                  | 641                 | 958                  | 695               | 335.2208481                      | 0.3199        | 182                    |
| 3   | 454                  | 628                 | 939                  | 681               | 327.6162162                      | 0.3188        | 180                    |
| 4   | 464                  | 641                 | 957                  | 695               | 335.2208481                      | 0.3228        | 182                    |
| 5   | 467                  | 646                 | 965                  | 700               | 337.7192982                      | 0.3226        | 183                    |
| 6   | 458                  | 635                 | 949                  | 689               | 331.6042781                      | 0.3201        | 181                    |
| 7   | 468                  | 647                 | 967                  | 701               | 338.8371278                      | 0.3240        | 183                    |
| 8   | 457                  | 634                 | 948                  | 688               | 330.4857143                      | 0.3187        | 181                    |
| 9   | 453                  | 627                 | 937                  | 680               | 326.4981949                      | 0.3174        | 179                    |
| 10  | 458                  | 635                 | 949                  | 689               | 331.6042781                      | 0.3201        | 181                    |
| 11  | 458                  | 635                 | 949                  | 689               | 331.6042781                      | 0.3201        | 181                    |

|    |     |     |     |     |             |        |     |
|----|-----|-----|-----|-----|-------------|--------|-----|
| 12 | 464 | 641 | 957 | 695 | 335.2208481 | 0.3228 | 182 |
| 13 | 456 | 631 | 943 | 684 | 329.7419355 | 0.3187 | 180 |
| 14 | 454 | 629 | 940 | 683 | 328.6247756 | 0.3202 | 180 |
| 15 | 454 | 629 | 940 | 683 | 328.6247756 | 0.3202 | 180 |
| 16 | 458 | 635 | 949 | 689 | 331.6042781 | 0.3201 | 181 |

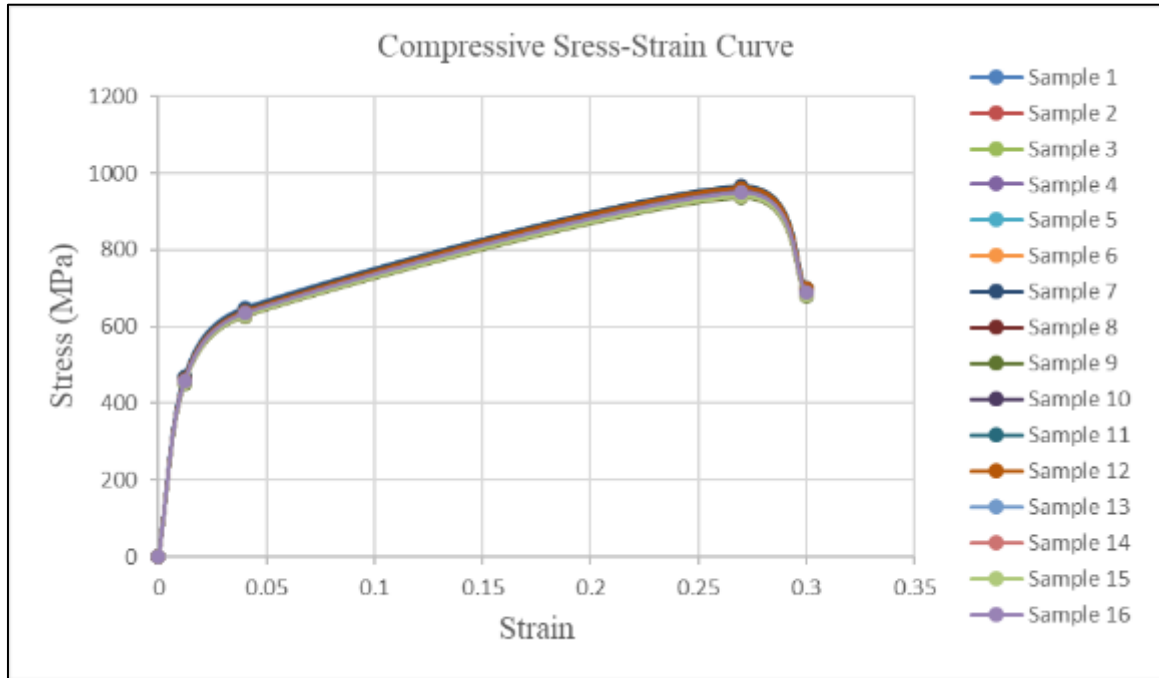


Figure 3 Compressive strength for test specimens

Table 4 Tensile Strength

| Run | Limit of Prop. (MPa) | Elastic Limit (0.2% offset (MPa)) | Tensile Strength MPa | Fracture Strength (MPa) | Strength Below Prop. Limit (MPa) | Elastic Modulus (GPa) | E |
|-----|----------------------|-----------------------------------|----------------------|-------------------------|----------------------------------|-----------------------|---|
| 1   | 311                  | 430                               | 785                  | 570                     | 275                              | 183                   |   |
| 2   | 309                  | 427                               | 780                  | 566                     | 273                              | 182                   |   |
| 3   | 303                  | 420                               | 765.3                | 555                     | 267                              | 180                   |   |
| 4   | 309                  | 427                               | 779.4                | 566                     | 273                              | 182                   |   |
| 5   | 311                  | 430                               | 786                  | 570                     | 275                              | 183                   |   |
| 6   | 306                  | 424                               | 773.3                | 561                     | 270                              | 181                   |   |
| 7   | 312                  | 431                               | 787.4                | 571                     | 276                              | 183                   |   |
| 8   | 305                  | 423                               | 772                  | 560                     | 269-                             | 181                   |   |
| 9   | 302                  | 418                               | 764                  | 554                     | 266                              | 179                   |   |
| 10  | 306                  | 424                               | 773.3                | 561                     | 270                              | 181                   |   |
| 11  | 306                  | 424                               | 773.3                | 561                     | 270                              | 181                   |   |
| 12  | 309                  | 427                               | 779.4                | 566                     | 273                              | 182                   |   |

|    |     |     |       |     |     |     |
|----|-----|-----|-------|-----|-----|-----|
| 13 | 304 | 421 | 769   | 558 | 269 | 180 |
| 14 | 303 | 420 | 767   | 557 | 268 | 180 |
| 15 | 303 | 420 | 767   | 557 | 268 | 180 |
| 16 | 306 | 424 | 773.3 | 561 | 270 | 181 |

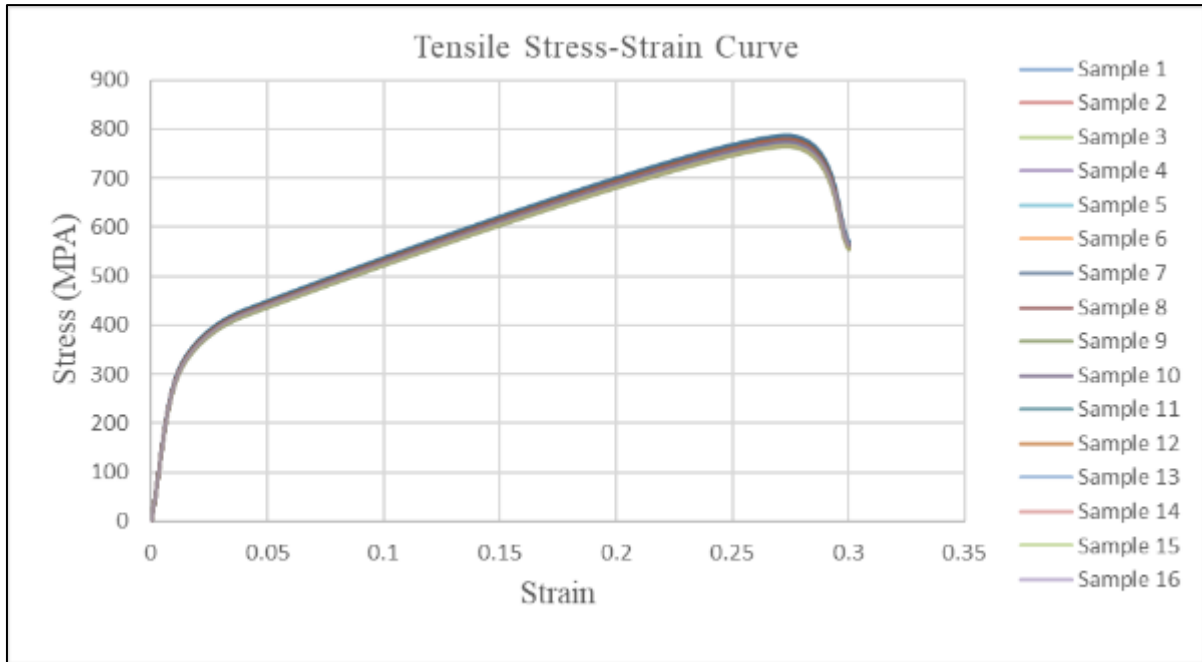


Figure 4 Stress-strain curve for the 16 test samples

### 5. Optimization

Optimization of the research results is as shown in table 5-6. For each responses, the value chosen is underlined and tagged selected.

Table 5 Compressive strength and Poisson ratio optimization (goal: maximize)

| Number | Al    | Mo    | Compressive Strength | Poisson Ratio | Desirability |          |
|--------|-------|-------|----------------------|---------------|--------------|----------|
| 1      | 3.300 | 1.440 | 969.048              | 0.324         | 0.995        | Selected |
| 2      | 3.300 | 1.434 | 968.933              | 0.324         | 0.993        |          |
| 3      | 3.286 | 1.440 | 968.850              | 0.324         | 0.992        |          |
| 4      | 3.259 | 1.440 | 968.473              | 0.324         | 0.985        |          |
| 5      | 3.252 | 1.440 | 968.380              | 0.324         | 0.983        |          |
| 6      | 3.130 | 1.440 | 966.851              | 0.323         | 0.950        |          |
| 7      | 3.073 | 1.440 | 966.227              | 0.323         | 0.930        |          |
| 8      | 2.977 | 1.440 | 965.278              | 0.323         | 0.896        |          |
| 9      | 2.577 | 1.440 | 962.914              | 0.321         | 0.765        |          |

**Table 6** Tensile strength optimization solutions (goal: maximize)

| Number | Al    | Mo    | Tensile Strength | Desirability |          |
|--------|-------|-------|------------------|--------------|----------|
| 1      | 3.300 | 1.440 | 787.425          | 0.994        | Selected |
| 2      | 3.300 | 1.434 | 787.302          | 0.990        |          |
| 3      | 3.300 | 1.428 | 787.195          | 0.987        |          |
| 4      | 3.300 | 1.399 | 786.601          | 0.967        |          |
| 5      | 3.167 | 1.440 | 786.970          | 0.948        |          |

**6. Comparison of the Mechanical Properties of the Research Alloy, Monel 400 and K-500**

**Table 7** Tensile and yield strengths of Molyb-Monel comparison with that of Monel 400, and K500

| Alloy       | Tensile Strength (MPa)    |       | Compressive Strength (MPa) |     | Young Modulus (GPa) |              |
|-------------|---------------------------|-------|----------------------------|-----|---------------------|--------------|
|             | Elastic Limit 0.2% offset | UTS   | Elastic Limit 0.2% offset  | UTS | E                   | Elongation % |
| Molyb-Monel | 431                       | 787.4 | 647                        | 967 | 183.3               | 30           |
| Monel 400   | 345                       | 620   | 508                        | 759 | 179                 | 48           |
| K-500       | 414                       | 758   | 621                        | 928 | 179                 | 35           |

**Table 8** Comparison of Elastic moduli and elongation

| Alloy       | Young Modulus (E)(GPa) | Bulk Modulus, K (GPa) | Shear Modulus, C (GPa) | Elongation (%) |
|-------------|------------------------|-----------------------|------------------------|----------------|
| Molyb-Monel | 183.3                  | 168.2                 | 69.4                   | 30             |
| Monel 400   | 179                    | 167                   | 69                     | 48             |
| K-500       | 179                    | 162                   | 68                     | 35             |

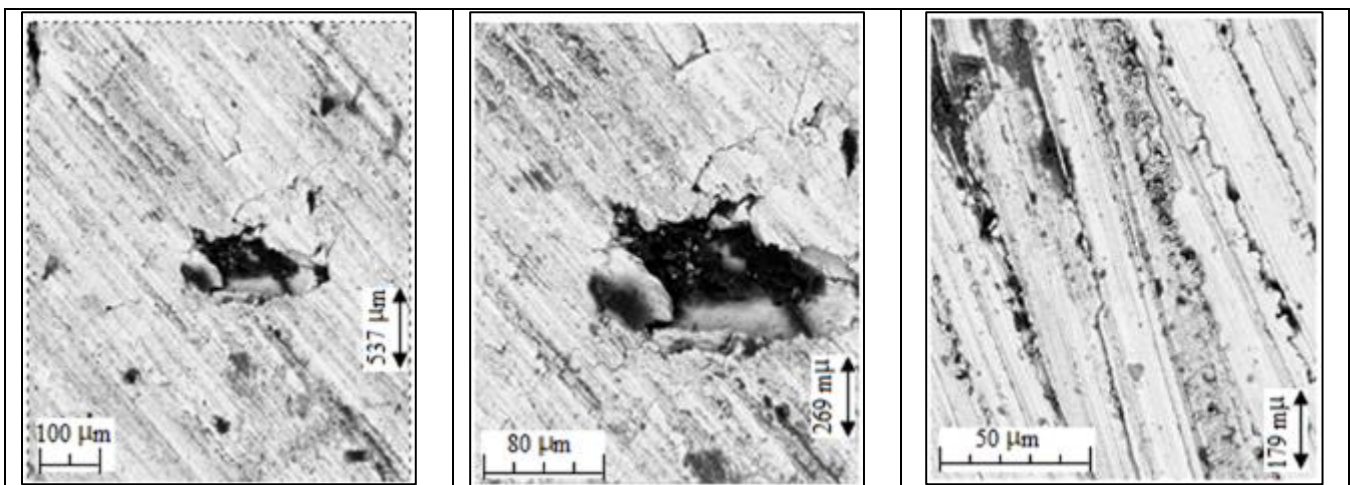


**Figure 5** (a and b) SEM analysis of research specimens showing olumnar, equiaxed grains structure; block particle Mo-C primary carbides. Magnification (a) 500x (b) 1000x (c) Columnar jagged grains, block particle (Mo-C) primary carbide. Magnification (1500x)

## 7. Discussion

Microstructural details of the test specimens under SEM investigation reveal single-phase interstitial solid solution with a face-centered cubic crystalline structure that contain block particles (Mo-C) primary carbide. The block particles (Mo-C) primary carbide are well ordered with uniform and visible homogeneous uniform distributions in intergranular and intragranular locations. Lattice grains exhibit proper order with visible twins (annealing twins) and stacking faults, fig. 5c. The block particles (Mo-C) primary carbides suggests presence of secondary phase however, it is not. This is because the solute weight percentage is greatly less than the requirement to exceed the solubility limit of the solvent. Research samples lattice grains is characterized with columnar and equiaxed particle structure (grains), which evidently reveal  $\langle 100 \rangle // CD$  and  $\langle 111 \rangle CD //$  orientation fibers, fig. 5. The  $\langle 110 \rangle // CD$  fiber texture include the  $\{001\} \langle 100 \rangle$  cube texture and  $\{110\} \langle 001 \rangle$  Goss texture. The  $\langle 111 \rangle // CD$  include  $\{112\} \langle 111 \rangle$  copper texture and  $\{110\} \langle 111 \rangle$  texture, fig. 5. Dislocation arrangements in the crystalline is planar in majority of the grains regions, with dislocation twins visible in the absence of any marked tendency for dislocation distribution along a properly defined planar array or pairing. Technically, this relates high stacking fault energy for the research alloy with absence of short-range order. It is worth mentioning that nickel has high stacking fault energy, which could decrease by alloying as in Ni-Cr base alloys. Besides having copper in substantive quantity in Monel 400 could reduce stacking fault energy. However, following the presence of very small quantities of alloying elements in Monel 400, nickel stacking fault energy remain not affected or reduced with copper addition. Thus stacking fault change in Ni-Cu matrix is most likely small. It is suffix to recall Raynor, and Silcock in their studies on some  $\gamma^1$  hardened alloys observed tangled dislocation arrangements in solution treated, and deformed condition. Both concluded such arrangements is due to the stacking fault energy of Monel metals.

In comparison to the solvent and k500, test samples showed higher resistance to deformation during testing. Greater energy is required to stress the specimens beyond their elastic limits during compression and tension (937-967 and 764-787.4) MPa. In addition, test specimen recorded elastic limit of (179-183.3) GPa. Notably in the elastic and plastic limit, test samples maintained appreciable (greater) resistance to plastic flow. Samples with higher molybdenum percentage maintained higher resistance to deformation and vice versa, tables 3 and 4. This behaviour essentially suggests adequate dissolution of the additives (Al and Mo) and its occupation of interstitial sites in the solvent crystal lattice. This no doubt characterized grain sizes refinement and creation of more grain boundaries. Grain refinement and increase in grain boundaries are notable to impede plastic deformation. Improvement in compressive and tensile strengths, Poisson ratio and elastic modulus of test specimens is due to the solutes (Al and Mo). Svea, et al had earlier studied the strengthening effect produced by grain size reduction and the blockage of dislocations by grain boundaries. Therefore, a fine-grained material is stronger than one that is coarse grained, since the former has a greater total grain boundary area to obstruct dislocation motion. This point to an important feature of microstructures because grain boundaries are frequently points of internal weakness along which failure by fracture or corrosion propagates through the interfacial network. Thus, the finer the grain sizes, more the grain boundaries, are a reflection of the higher mechanical properties.

Degree of grain refinement created by alloying is a reference to the solubility of the solute in the solvent. Solute high solubility in the solvent is because of the distance between the former and later in the electrochemical series (periodic table) of elements, and the comparatively smaller size of the solute (4.74) % in the solvent (95.26) %. Consequently, the solute dissolve into the solvent adequately filling vacancies in the solvent crystal lattice to form a single-phase interstitial solid solution. In addition, fine grains observations in the research alloy obviously hinge on the concept that alloys are technically mixture of two or more elements combined in liquid. This is possible because most elements are soluble in each other in the liquid state, forming randomly mixed solution. However, solid metals have restricted capacity to take other elements into solution, so they have limited solubility. This results in alloys to consist of two or more different phases. In cases where the elements in an alloy are soluble in each other, a single alloy (solid solution) forms. This occurs mostly where the elements have similar atomic sizes and crystal structures. Nevertheless, in cases where the elements have different sizes like in steel, i.e. an iron-based alloy, where the majority element is iron. Then if the solute atoms are very much smaller in comparison with that of the solvent, e.g. C in solvent of iron, there is the possibility to form a solid solution, where the additives atoms fit into some of the gaps (vacancies) in the lattice of the solvent. Solute occupation of vacancies in the solvent microstructure provide barrier to dislocation motion. This increase the Peierls-Nabarro stress (stress required to move dislocations) thus improve the research alloy resistance to deformation. This is possible since restriction of dislocation motion is one method of strengthening metals. Alloy strengthening is achievable by either generating internal stress that oppose dislocation motion, or by placing particles in their path, which require them to cut or loop the particles. Consequently, solid solution hardening provides means for effective strengthening and hardening of metals (in other words, grain boundaries act as barriers to dislocation motion during plastic deformation). The principle basics is that when solute-alloying atoms dissolves in a solid metal, it acts as an atomic-sized obstacle to dislocation motion, and strengthen the metal.

Strengthening effect relies on the nature of interactions of the dislocation with the solute atoms. Most often, two general interactions exist which are considered. One is of a chemical nature in which the difference in chemical bonding between solute atoms and solvent atoms reflects in the difference in their elastic shear moduli. This effects a change in the dislocation-atom interaction. In other words, the foremost reason grain boundaries act as barriers to dislocation motion during plastic deformation is because grains are of different crystallographic orientations. Therefore, as dislocation pass from one grain to another its direction of motion alters. Besides, as the mis-orientation between the grains increases, the process is restricted the more, fig. 5. The other interaction is an elastic nature in which if the size of the solute atoms differ from those of the substance (solvent) atoms, then a misfit strain field forms around the solute atom that interacts with the strain field of the dislocations. In other words, atomic disorder inside a grain boundary region triggers discontinuity of slip planes from one grain into the other. Therefore, the boundaries separating two different phases also constitute barriers to dislocations. This behavior apply for strengthening metallic materials with complex multi-phase(s). It accounts for improvements in the compression and tensile strengths of the research alloy. Notably increase and decrease in molybdenum reflects corresponding increase and decrease in strengths (compressive and tensile) and Poisson ratio, tables 3 and 4. Property improvement in the research alloy reveal increase of (4.2, 27.4)% and (4, 27)% in compressive and tensile strengths, (2.4 and 0)% in elastic modulus and Poisson ratio over Monel 400 and k500, tables 7 and 8. This point to a vital attribute of microstructures because grain boundaries are frequently points of internal weakness on which failure by fracture or corrosion will grow or spread through materials interfacial network. Thus, the finer the grain sizes, more is the grain boundaries, and is a reflection of the higher mechanical properties. Fine-grained materials are stronger (having stronger bonding intermolecular force) than one that is coarse grained, because the former has more numbers of grain boundary area that will obstruct dislocation motion. Molybdenum been a refractory material and a genuine all-rounder in metallurgical matters impede dislocation motion, which provides for improvement in both compressive strength, tensile strength and elastic modulus. In addition, it annulled the need for age hardening thereby reducing the cost of mechanical processing required for further strength improvements unlike as is obtainable in k500. Optimization of the solute response in the solvent reveal (3.30 and 1.44) % of (Al and Mo) will produce maximum compressive and tensile strengths (969 and 787.4) MPa, elastic modulus of (183.7) GPa and Poisson ratio of 0.324, tables 3, 4, 5 and 6. Hence, increase in molybdenum percentage reflects higher strengths and elastic modulus, tables 3 and 4.

---

## 8. Conclusion

The solute (Al and Mo) are highly soluble in the solvent enabling both to occupy interstitial sites (vacancies) in the solvent crystal lattice to form single-phase solid solution with a face-centered cubic crystalline structure. The additive (Mo) formed Mo-C block primary particles with well-ordered lattice grains and visible annealing twins, and stacking faults. These block particles are distributed both in intergranular and intragranular locations. This however, does not suggests the presence of secondary phase. Microstructural changes created by (Al and Mo) in the solvent provided for grain refinement and more grain boundaries, which improved the research alloy Peierls-Nabarro stress and subsequent higher compressive and tensile strengths and elastic modulus in comparison to Monel 400 and or k500. In addition, the additive (Mo) been a refractory material, exclude the need for age hardening thereby reducing cost of mechanical processing required for further improvement in strengths in the research alloy.

### *Recommendations*

Alloying is a vital and cost effective technology capable of conforming materials to different applications and service environments. In applications where outstanding strengths (compressive and tensile) is a crucial consideration not weight to strength ratio especially at elevated temperature environments, Monel 400 strengthened with (Al and Mo) is a preference to Monel 400 and or k500.

---

## Compliance with ethical standards

### *Disclosure of conflict of interest*

No conflict of interest to be disclosed.

---

## References

- [1] Aalco (2024). Aluminum Alloy Specifications. Aalco Metals Ltd Parkway House, Unit 6 Parkway Industrial Estate, Wednesbury WS10 7WP

- [2] A. G. Kostryzhev, O. O. Marenych, Z. Pan, H. Li & S. van Duin (2023). Strengthening Mechanisms in Monel K500 alloyed with Al and Ti. *J Mater Sci. of Metals and Corrosion* 58:4150–4164.
- [3] Aldrich (2007). *Advanced Metals and Alloys*. Journal of Material Matters vol. 2, No. 4, pp 1-28. Published by Aldrich Chemical Co. Inc.
- [4] Aleksander V. Abramov, Ruslan R. Alimgulov, Anastasia I. Trubcheninova, Arkadiy Yu. Zhilyakov, Sergey V. Belikov, Vladimir A. Volkovich & Ilya B. Polovov (2023). Corrosion of Molybdenum-Based and Ni–Mo Alloys in Liquid Bismuth–Lithium Alloy. *Materials. Metals* 13, 366 pp 1-10. [https:// doi.org/10.3390/met13020366](https://doi.org/10.3390/met13020366)
- [5] Anaemeje J. C., Owuama K. C., Okafor O. C., Madu K. E. (2022). Determination of a Suitable Retrofit of R-134A Using Refrigerant Blends of R290 and R600 Aided by an Optimization Technique. *Journal of Engineering Sciences* vol. 9 (1), pp G1-G7, doi: 10.21272/jes.2022.9 (1).g1
- [6] Ashby, M. F. (1999). *Materials Selection in Mechanical Design*, Second Edition. Butterworth Heinemann Inc., New Delhi, India.
- [7] Ashby, M. F. (2003). *Materials Selection Report*. Unified Engineering Inc. USA.
- [8] ASTM (2003). *Standard Test Methods for Tension Testing of Metallic Materials*. American Society for Testing and Materials (ASTM) Standards International E8-03.
- [9] ASTM (2019). *Standard Test Methods of Compression Testing of Metallic Materials at Room Temperature*. American Society for Testing and Materials International E9–E19.
- [10] ASTM (2013). *Standard Test Methods for Tension Testing of Metallic Materials*. American Society for Testing and Materials (ASTM) Standards International E8/E8M-13a.
- [11] Author-Shiv Om Kumar, Vineeta Shukla & Sanjeev Kumar Srivastava (2019). Role of Electronegativity on the Bulk modulus, Magnetic Moment and Band gap of Co<sub>2</sub>MnAl Based Heusler Alloys. *Journal of Science: Advanced materials and Devices* vol. 4, pp 159-162. Published by Elsevier B.V.
- [12] B. Mirzakhani, Y. Payandeh, H. Talebi & M. Maleki (2020). Significant Increase in Strength and Elongation of Al-3.7Cu-1Mg Alloy via Short Age-Treatment Cycle. *Iranian Journal of Materials Science and Engineering* vol. 17, No. 3, pp 30-39.
- [13] Bhanu Teja Chintalapudi, Chaithanya Baba Gonuguntla, Manideep Pothuri, Jamini Kant S.H.V and Arief Pathan & Raj Kumar Pittala (2017). Investigation of Mechanical Properties of Duralumin Sandwich Hybrid Composite using E-glass Fiber. *International Journal of Mechanical Engineering and Technology*, Vol. 8, Issue 5, pp. 425–431, IAEME Publication.
- [14] C. C. Clickner J. W. Ekin N. Cheggour, C. L. H. Thieme, Y. Qiao, Y. -Y. Xie, A. Goyal. (2006). Mechanical Properties of Pure Ni and Ni-Alloy Substrate Materials for Y–Ba–Cu–O Coated Superconductors. *Cryogenics* vol. 46, pp 432–438. Published by Elsevier Ltd.
- [15] Dorothy Ofoha, Mars Anaekwe, Josiah Owolabi, Ibrahim Musa & Ayodele Badmus (2019). *Research Project Manual and Format of Writing and Presenting a Research Report. A Research Guide for Undergraduate and Postgraduate Students*. Nigeria Open University Victoria Island, Lagos.
- [16] Emilija Ilic, Ainhoa Pardo, Roland Hauert, Patrik Schmutz & Stefano Mischler (2019). Silicon Corrosion in Neutral Media: The Influence of Confined Geometries and Crevice Corrosion in Simulated Physiological Solutions. *Journal of the Electrochemical Society*, 166 (6) C125-C133.
- [17] H. M. Ledbetter & R. P. Reed (2009). *Elastic Properties of Metals and Alloys, I. Iron, Nickel and Iron-Nickel Alloys*. *Journal of Physical and Chemical Reference Data* 2, vol. 2, No. 3 pp. 531-617. Published by AIP Publishing.
- [18] John A. Shields, Jr. PhD. (2013). *Applications of Molybdenum Metal and its Alloys*. International Molybdenum Association (IMOA). London UK. Second Completely revised edition. ISBN 978-1-907470-30-1 [www.imoa.info](http://www.imoa.info), [info@imoa.info](mailto:info@imoa.info)
- [19] ISO (2009). *Materials Tensile Testing, Part 1. Methods of Test at Room Temperature*. First edition ISO-6892-1:2009(E). International Standards Organization.
- [20] Ivan Richardson (2016). *Guide to Nickel Aluminium Bronze for Engineers*. Copper Development Association Publication No 222. [info@copperalliance](mailto:info@copperalliance).

- [21] Iwuoha, A.U., Swift, O.N.K. and Owuama, K.C. (2013). Localised Corrosion Susceptibility of AISI 316L Stainless Steel Welded Joints in High Temperature Alkaline environments. *Journal of Sustainable Technology*, vol. 4(2), pp 25-33.
- [22] Juan Liu, Emrys Tennessen, Jianwei Miao, Yu Huang, James M. Rondinelli, & Hendrik Heinz (2018). Understanding Chemical Bonding in Alloys and the Representation in Atomistic Simulations. *The Journal of Physical Chemistry C* 122, pp 14996–15009. American Chemical Society (ACS).
- [23] Khlystov, Lizardo, Matsushita & Zheng (2013). Uniaxial Tension and Compression Testing of Materials. Published by Lab. Report Inc. New Delhi India.
- [24] M. Ashby & D. Cebon (1993). Material Selection in Mechanical Design. *Journal of De Physique IV Proceeding* vol. 03 (07), pp C7-1-C7-9.
- [25] Patrick C. Okonji, Chidozie C. Nwobi-Okoye, Kennedy C. Owuama (2019). Experimental Study of Optimization of Dry Compressive Strength of Groundnut Shell Ash and Ant Hill Powder-Bonded Sand for Foundry Application. *World Journal of Innovative Research (WJIR)*, Vol. 6, Issue 6, pp 23-28, ISSN: 2454-8236
- [26] Plansee (2023). Molybdenum Material Properties and Alloys. Published by Plansee SE Metallwerk-Plansee-Str. 71 6600 Reutte Austria. [www.plansee.com](http://www.plansee.com)
- [27] Pradeep L. Menezes, Kishore and Satish V. Kailas (2007). Influence of Surface Textures During Metal Forming. *International joint Tribology Conference*, pp 713-715. American Society of Mechanical Engineers (ASME).
- [28] Rajput, R. K. (2010). *Material Science, and Engineering Third Edition (Reprint)* pp. 1-349, 387-555, and 985-996. Published by S.K. Kataria & Sons, Nai Sarak, Delhi, India.
- [29] Rajput, R. K. (2008). *Strength of Materials (Mechanics of Solids) Revised Edition with Reprint and Corrections* pp. 27-29, 1389-1419. Published by S. Chand & Company Ltd., Ram Nagar, India.
- [30] Rizar GÜRBUZ (2005). Tension Test Met E206 Materials Laboratory Report. Department of Materials and Metallurgical Engineering, University of Indonesia.
- [31] Tomohiro Takida, H. Kurushita, Mamoru Mabuchi Tadashi Igarashi, Yoshiharu Doi and Nagae Takekezu (2004). Mechanical Properties of Fine-Grained, Sintered Molybdenum Alloys with Dispersed Particles Developed by Mechanical Alloying. *Materials Transactions* Vol. 45, No. 1, pp. 143-148.
- [32] Xiao Dong, Artem R. Oganov, Haixu Cuic, Xiang-Feng Zhou, & Hui-Tian Wang. (2022). Electronegativity and Chemical Hardness of Elements under Pressure. *PNAS* Vol. 119, No. 10, pp 1-18 <https://doi.org/10.1073/pnas.2117416119>.